BMC Microbiology

RESEARCH

Open Access

Interactions between phytoplankton and bacterioplankton communities in Caohai plateau lake, revealed by environmental DNA metagenomics

Yunchuan Long[1,2*], Jin Guo[1*], Liangliang Dai[1] and Juan Jiang[1]

Abstract

Phytoplankton-bacterioplankton interactions critically influence aquatic ecosystem stability, yet their dynamics remain poorly understood in eutrophic plateau lakes. This study employed environmental DNA (eDNA) metagenomics to investigate these cross-kingdom relationships in Caohai Plateau Lake, a vulnerable wetland undergoing macrophyte-to-algae regime shifts, integrating correlation analysis, niche overlap, redundancy analysis (RDA), co-occurrence networks, and neutral community model (NCM). A total of 331 phytoplankton species across 10 phyla were characterized in the phytoplankton community, dominated by Cyanophyta with *Microcystis* as the representative genus, while bacterioplankton communities were primarily structured by Proteobacteria and *Sphingomonas*. The assembly of phytoplankton community was primarily driven by stochastic processes (R^2>0.90). Co-occurrence network analysis showed phytoplankton interactions were dominated by positive effects (84.25%), whereas bacterioplankton networks exhibited balanced positive and negative effects. Metabolic specialization emerged through LEfSe analysis: phytoplankton specialized in photosynthesis and carbon storage, while bacterioplankton dominated anaerobic respiration (propanoate metabolism). The positive interactions were more prevalent than negative ones; combined with the metabolic complementarity of phytoplankton and bacterioplankton, this suggests that mutualism is more dominant than competition in cross-kingdom interactions. High niche overlap under sufficient nutrients (TP) facilitated species coexistence of phytoplankton and bacterioplankton by minimizing resource competition, thereby promoting stochastic community assembly, while keystone taxa (*Cyanothece*, *Sphingobium*) mediated ecosystem stability. This work demonstrates that nutrient enrichment promote stochastic assembly in eutrophic plateau lakes.

Keywords Phytoplankton, Bacterioplankton, Environmental DNA, Plateau wetland, Community assembly

*Correspondence:
Yunchuan Long
sculyc@163.com
Jin Guo
guojinjudy@163.com

Full list of author information is available at the end of the article

Graphical abstract

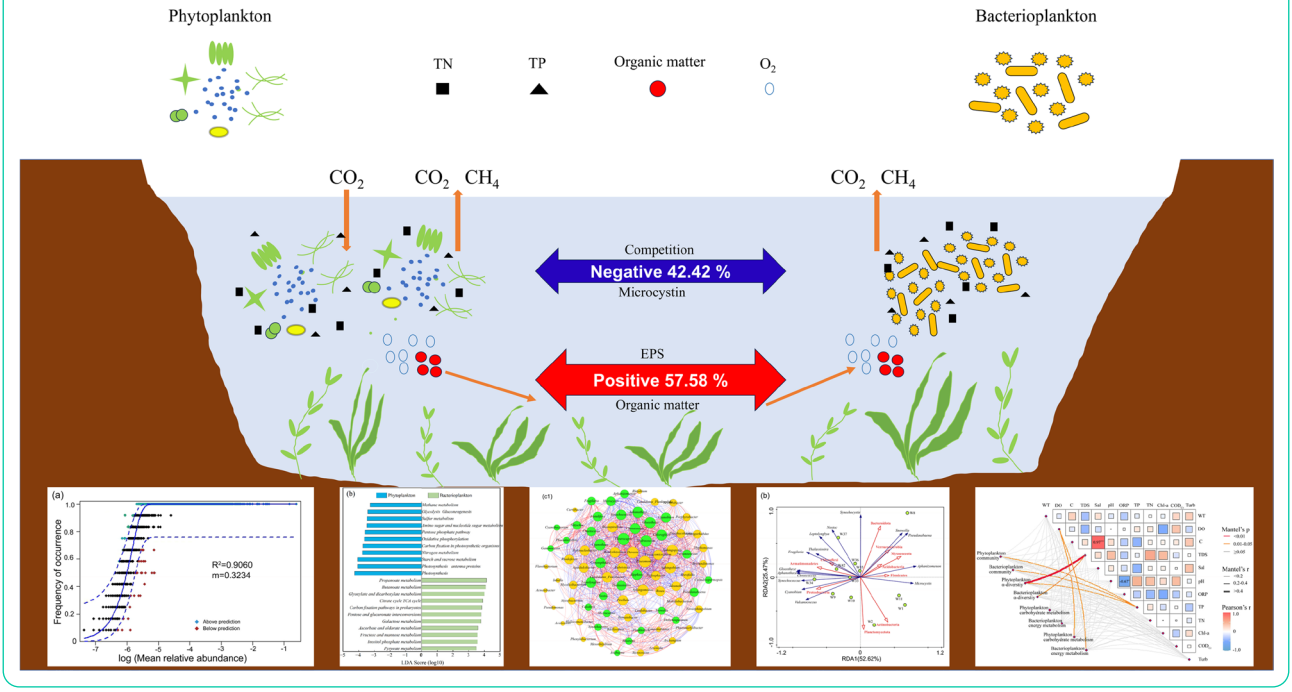

Introduction

Phytoplankton represent a crucial source of primary production and constitute the foundation of aquatic food webs [25, 26]. They exhibit rapid responsiveness to fluctuations in environmental factors such as pH, dissolved oxygen (DO), and nutrient concentrations [23, 55]. Consequently, they are often employed as environmental indicators, providing essential references for the conditions of water quality and the conservation of aquatic ecosystems [53]. Traditionally, microscopic observation based on cell morphology has been the predominant method for assessing phytoplankton biodiversity [13]. However, this technique is time-consuming and requires a comprehensive understanding of phytoplankton morphology and taxonomy. More importantly, accurately identifying small, rare, or cryptic phytoplankton species using microscopic methods poses considerable challenges [14].

Bacterioplankton play a crucial role in the biodiversity and biogeochemical cycles within aquatic ecosystems, as they quantitatively dominate freshwater planktonic communities [48]. Phytoplankton and bacterioplankton dynamics are thought to be closely linked in aquatic ecosystems, with frequent correlations observed between their biomass levels [34]. Phytoplankton fix carbon and release dissolved organic matter (DOM) through photosynthesis, while bacterioplankton participate in the cycling of carbon, nitrogen, and phosphorus by decomposing DOM [3]. They interact through various mechanisms, including mutualism, symbiosis, parasitism, competition, and non-symbiotic interactions [5]. The interaction between phytoplankton and bacterioplankton is the core link of material cycling and energy flow in lake ecosystems, which plays an important role in maintaining the structure and function of lake ecosystems [33]. Nevertheless, there is a paucity of information regarding the interactions between phytoplankton and bacterioplankton communities, as well as the underlying mechanisms, in plateau lakes [55].

In recent years, environmental DNA (eDNA) analysis has emerged as a powerful and sensitive tool for monitoring aquatic microbial biodiversity [36, 53]. eDNA metagenomics integrates information from multiple genomic markers and assembles longer contigs, thereby offering higher taxonomic resolution compared to eDNA metabarcoding, particularly for small, rare, or cryptic species [2, 40]. This is of critical advantage in eutrophic lakes, where micro-phytoplankton play vital ecological roles. Although eDNA metagenomics has been validated in freshwater zooplankton studies [30], its application to phytoplankton-bacterioplankton interactions in plateau lakes remains scarce, limiting a comprehensive understanding of cross-kingdom relationships in these unique ecosystems.

With the effects of global warming and human activities, lakes are often faced with threats such as eutrophication and algal blooms [46]. Algal blooms in lakes are a major hazard worldwide. Thus, understanding the

mechanism of phytoplankton and bacterioplankton community formation in aquatic ecosystems constitutes an essential condition for effective prevention of algal blooms and scientific management of aquatic ecosystems [51]. Deterministic and stochastic processes represent fundamental mechanisms underlying the assembly of microbial communities [53]. Based on deterministic processes, both biotic factors (such as species interactions) and abiotic factors (such as environmental filters) exert prominent roles in the structuring of microbial communities [54]. Based on stochastic processes, the birth, death, diffusion, and ecological drift of all species are regarded as the major determinants of microbial community dynamics [14]. However, it remains ambiguous how stochastic and deterministic processes influence the community assembly of phytoplankton and bacterioplankton in eutrophic plateau karst lakes.

Plateau lakes, as sensitive indicators of global climate change, are increasingly experiencing a "macrophyte-to-algae" regime shift driven by eutrophication, which represents a central challenge in contemporary ecological conservation [42]. The interaction between phytoplankton and bacterioplankton plays a crucial role in regulating lake biogeochemical cycles and maintaining ecosystem stability. Focusing on Caohai Lake (hereafter referred to as Caohai), a plateau lake system currently undergoing eutrophication [21], this study employed eDNA metagenomic approaches to: (1) identify the community composition and assembly mechanisms of phytoplankton and bacterioplankton in eutrophic plateau lakes; (2) reveal the patterns of cross-kingdom interaction between phytoplankton and bacterioplankton, along with the key environmental drivers and underlying metabolic and niche characteristic.

Materials and methods

Study area and sampling

Caohai (104∘12′–104∘ 18′ E, 26∘ 49′–26∘53′N), located in the southwest of Weining County, Guizhou Province, southwest China, is one of three plateau freshwater lakes in China and a primary wintering site of *Grus nigricollis*, an endemic plateau bird in China. It has an average temperature of 10.5 ℃ and an altitude of 2170 m above sea level. With an average depth of 2.0 m and abundant aquatic vegetation, Caohai is regarded as a typical shallow lake ecosystem [27, 42]. In this study, 12 water samples were collected from Caohai in July 2023 and labeled as W01-W12. The sampling sites, distributed in a grid pattern, are presented in Fig. S1. Surface water was collected at a depth of 0.5 m using a plexiglass water sampler, which was sterilized with 75% ethanol before use. At each site, five 1-L subsamples were collected and combined in equal volumes to yield a homogeneous composite sample. All samples were immediately stored at a low temperature and transported to the laboratory. A 0.5-L aliquot from each water sample was filtered through a 0.45 μm pore-sized membrane to capture phytoplankton, and another 0.5-L aliquot was filtered through a 0.22 μm pore-sized membrane to capture bacterioplankton. The filter membranes were then collected, placed in 15 mL sterile centrifuge tubes, and stored at ultra-low temperatures for eDNA extraction as soon as possible.

Environmental data collection

The pH, total dissolved solids (TDS), water temperature (WT), dissolved oxygen (DO), conductivity (C), and salinity (Sal) of the water body were measured in situ using a portable multi-parameter water quality analyzer (YSI Professional Plus, USA). The remaining physicochemical parameters were tested in the laboratory. The physicochemical properties of the overlying water were measured according to the Chinese standard method for surface water (GB3838-2002). Turbidity was measured by a turbidimeter. Chlorophyll a (Chl-a) was determined by ethanol extraction [7]. Total nitrogen (TN) was determined by potassium persulfate oxidation ultraviolet spectrophotometry. Total phosphorus (TP) was determined by molybdenum antimony anti-spectrophotometry. Chemical oxygen demand (COD_{Cr}) was determined using the potassium dichromate index method.

Gene extraction and analysis

Total eDNA was extracted using the FastDNATM Spin Kit for Soil extraction kit (MP Biomedicals) following the manufacturer's instructions, with nuclease-free distilled water serving as a negative control. The integrity of the extracted DNA was checked by 1% agarose gel electrophoresis. The purity and concentration of the eDNA were measured by a NanoDrop2000 spectrophotometer and a Quantus fluorometer (Picogreen), respectively. A metagenomic sequencing library was established and sequenced using the PE150 paired-end strategy on the Illumina Novaseq 6000 sequencing platform at Majorbio Bio-Pharm Technology Co., Ltd. (Shanghai, China) [52]. The raw sequencing data underwent quality control using fastp v0.20.0 software [27]. Adapter sequences at the end of the reads were trimmed, and reads with an average quality score below 20 or a length less than 50 bp were discarded, retaining only high-quality reads. Sequence assembly was performed using Megahit v1.1.2 [40], and contigs longer than 300 bp were selected for further analysis. Open reading frame (ORF) prediction of the assembled contigs was conducted using Prodiga v2.6.3, and the genes with nucleic acid lengths of 100 bp or more were selected, which were subsequently translated into amino acid sequences [8]. The predicted gene sequences from each sample were clustered using CD-HIT v4.6.1 with a similarity threshold of ≥ 0.9 and a coverage threshold

of ≥ 0.9 [57]. The longest gene in each cluster was chosen as the representative sequence to construct a non-redundant gene set. Gene abundance information and quantification in each sample were performed using SOAP aligner software with a similarity threshold of ≥ 0.95 [40]. To determine species information at each taxonomic level, Diamond v0.8.35 [20] was used to perform BLASTP comparisons of the non-redundant gene set against the NR database (with an E-value cutoff set at 1e-5). The abundance of species was calculated by summing the gene abundances corresponding to each species. The raw sequences were deposited in the NCBI Sequence Read Archive (SRA) database under BioProject PRJNA1243597.

Data analyses

Microsoft Excel 2019, SPSS 23.0, and R (v4.4.1) were used for data analysis, and Origin 2021 was used for graphing. Metabolism predictions of phytoplankton and bacterioplankton were conducted using the KEGG (Kyoto Encyclopedia of Genes and Genomes) database. The relative importance of stochastic processes in shaping phytoplankton and bacterioplankton community structure was assessed using a neutral community model (NCM) with "MicECO" package in R [6]. The activity of carbohydrate metabolism and energy metabolism pathways in bacterioplankton and phytoplankton was determined by linear discriminant analysis (LDA) effect size (LEFSe), with a threshold of LDA scores >3.0 [27]. Network analysis was performed using the "Hmisc" package in R and visualized with Gephi (v0.9.3) to delineate the interspecific interactions of phytoplankton and bacterioplankton community [54]. Based on the inferred within-module connectivity (Zi) and among-module connectivity (Pi) values, nodes in a network were categorized into four distinct topological roles: network hubs, module hubs, connectors, or peripherals [7]. The Mantel test (run with 999 permutations) was applied to evaluate the relationship between communities and environmental variables using the "vegan" package in R [39]. Niche overlap was calculated using the "spaa" package in R [18].

Results

Environmental characteristics of Caohai

The water temperatures in Caohai ranged from 21.00 to 21.90 °C, while pH values varied from 7.67 to 8.34. The concentration of DO fluctuated between 5.42 and 6.27 mg/L, with an average of 5.78 mg/L. The concentration of TDS ranged from 263.90 to 375.60 mg/L. The concentrations of TP and TN were 0.08 to 0.12 mg/L and 1.56 to 2.28 mg/L, respectively. The concentration of COD_{Cr} ranged from 10.46 to 41.14 mg/L, with an average of 24.51 mg/L. The turbidity concentration varied from 4.00 to 11.40 NTU. The concentration of Chl-a ranged from 12.00 to 16.00 μg/L with an average of 13.58 μg/L. Detailed information on the environmental characteristics is provided in the Supplemental file (Table S1).

Community characteristics of phytoplankton and bacterioplankton

331 species of phytoplankton were identified by eDNA metagenomics, distributed across 10 phyla and 197 genera. Based on relative abundance (>1%), the phytoplankton phyla were ranked as follows: Cyanophyta, Bacillariophyta, Chlorophyta, and Euglenozoa, as illustrated in Fig. 1a. Notably, Cyanophyta was the dominant phylum in all samples. At the genus level, the predominant genera were primarily *Microcystis*, *Cyanobium*, and *Synechococcus* (Fig. 1b). The relative abundance of *Microcystis* was 40.43% ± 8.87%. *Cyanobium* showed a relative abundance of 12.31% ± 2.64%, while *Synechococcus* exhibited a relative abundance of 8.90% ± 2.05%. The relative abundance of the bacterioplankton community in Caohai is shown in Fig. 1c and d. At the phylum level, the composition was primarily dominated by Proteobacteria, Bacteroidota (formerly Bacteroidetes), and Actinobacteria (Fig. 1c). At the genus level, the dominant genera were primarily *Sphingomonas*, *Erythrobacter*, and *Hyphomonas* (Fig. 1d).

Prediction of metabolisms of phytoplankton and bacterioplankton

Metabolic prediction revealed major pathways related to global and overview maps, carbohydrate metabolism, and energy metabolism in phytoplankton (Fig. S2a) and bacterioplankton (Fig. S2b). Given that carbohydrate and energy metabolism are fundamental to metabolic processes and essential for sustaining vital cellular functions, the associated pathways were further examined (Fig. S2c–d). Relatively featured pathways were identified in phytoplankton metabolism: in energy metabolism, oxidative phosphorylation (24.89%), carbon fixation pathways in prokaryotes (14.19%), and photosynthesis (13.81%); in carbohydrate metabolism: amino sugar and nucleotide sugar metabolism (14.30%), pyruvate metabolism (13.35%), and glycolysis/gluconeogenesis (12.35%). For bacterioplankton metabolism, in energy metabolism, oxidative phosphorylation (27.79%) was the most prominent, followed by carbon fixation pathways in prokaryotes (20.80%) and methane metabolism (14.65%). In carbohydrate metabolism, pyruvate metabolism (12.53%) was the most representative, followed by amino sugar and nucleotide sugar metabolism (11.91%), and glyoxylate and dicarboxylate metabolism (11.96%).

Principal components analysis (PCA) displayed significant differences in carbohydrate metabolism and energy metabolism pathways between bacterioplankton and phytoplankton (Fig. 2a). Furthermore, LEfSe

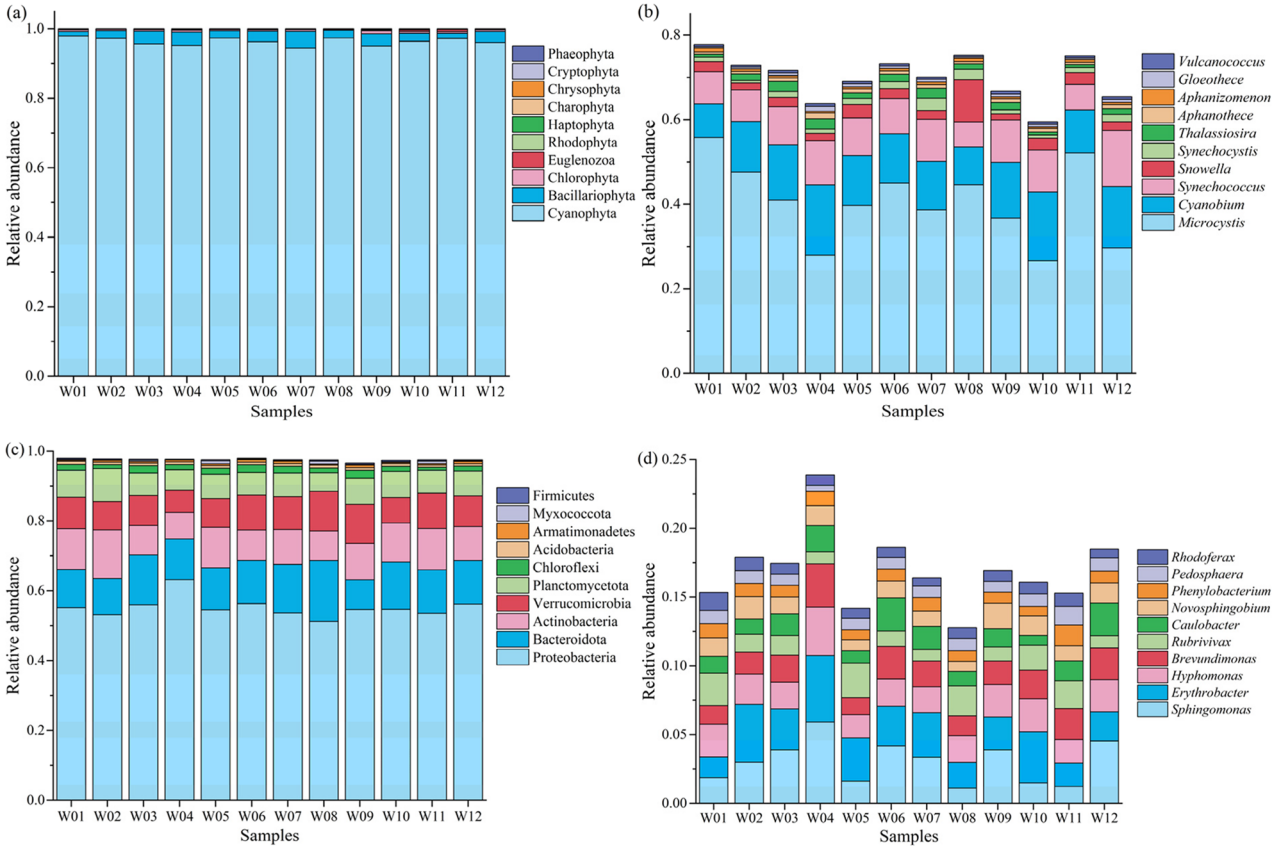

Fig. 1 Community structure of phytoplankton in Caohai at the phylum (**a**) and genus (**b**) levels, and of bacterioplankton at the phylum (**c**) and genus (**d**) levels. The data displayed are based on the relative abundances of the top 10 phyla and genera

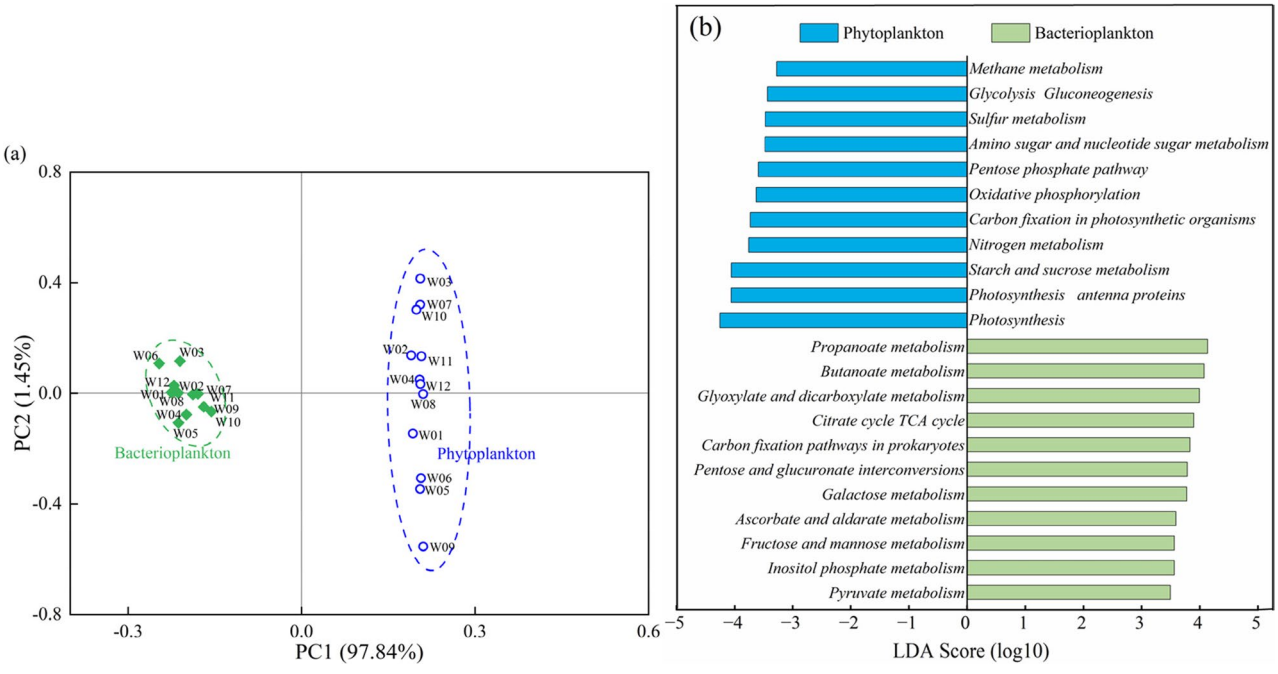

Fig. 2 (**a**) PCA analysis of carbohydrate and energy metabolism pathways in phytoplankton and bacterioplankton communities from Caohai, (**b**) LEfSe analysis identifies differentially abundant features of carbohydrate and energy metabolism between phytoplankton and bacterioplankton

analysis revealed that phytoplankton exhibited activity in photosynthesis, photosynthesis antenna proteins, and starch and sucrose metabolisms (Fig. 2b). In contrast, bacterioplankton primarily showed activity in propanoate metabolism, butanoate metabolism, glyoxylate, and dicarboxylate metabolism.

Community assembly of phytoplankton and bacterioplankton

The Sloan NCM estimated the role of stochasticity in both phytoplankton (Fig. 3a) and bacterioplankton (Fig. 3b) communities. The NCM model demonstrated high predictive accuracy, with R^2 values of 90.60% for phytoplankton and 88.74% for bacterioplankton communities. This suggested that stochastic processes exerted a stronger influence than deterministic processes on the community structure of both phytoplankton and bacterioplankton in Caohai. Notably, many taxa, particularly in bacterioplankton, fell outside the 95% confidence interval (CI) of the model (Fig. 3b), indicating that deterministic factors (such as ecological niche differentiation, environmental selection) likely played a more important role for these groups. The m value in the phytoplankton community (0.3234) was close to that in the bacterioplankton community (0.3211), indicating that their species dispersal patterns were comparable.

The phytoplankton and bacterioplankton genera with a relative abundance of more than 0.1% were selected to construct the co-occurrence network (Fig. 4a-f). The number of nodes in the phytoplankton (Fig. 4a) and bacterioplankton networks (Fig. 4b) at the genus level were 34 and 47, respectively, and their edge numbers were 273 and 332, respectively. These results suggest that the bacterioplankton network might be more complex than the phytoplankton network at the genus level. In the phytoplankton networks, the majority of interactions were positively associated with one another, accounting for 84.25%. In contrast, in the bacterioplankton network, the number of positive interactions was nearly equal to that of negative interactions (51.51% vs. 48.49%). The key taxa in the phytoplankton community were *Cyanothece*, which exhibited the highest number of edges, while *Sphingobium*, *Sphingopyxis*, and *Devosia* emerged as the key taxa in the bacterioplankton community. The phytoplankton-bacterioplankton network (Fig. 4c) consisted of 81 nodes and 1141 edges (57.58% positive and 42.42% negative). *Devosia* and *Pleurocapsa* had the highest number of edges, followed by *Roseomonas*, *Hydrococcus*, and *Sphingopyxis*. *Rubrivivax*, *Polynucleobacter*, and *Sphingomonas* were the most influential bacterioplankton on phytoplankton. *Rubrivivax* and *Polynucleobacter* interacted with 21 genera of phytoplankton, accounting for 61.76% of the total phytoplankton, and 90.47% and 95.23% of these interactions had negative effects, respectively. *Sphingomonas* interacted with 20 phytoplankton genera, exerting positive effects on 17 genera, including *Gloeothece*, and negative effects on 3 genera, such as *Snowella*.

The Zi (within-module connectivity) and Pi (among-module connectivity) values of the dominant genera in three networks (phytoplankton network, bacterioplankton network, and phytoplankton-bacterioplankton network) are displayed in Fig. 4d-f. As predicted by network theory, connectors may function similarly to keystone taxa in a community. In the phytoplankton network, the putative keystone genera were *Cyanothece*, *Calothrix*, *Crocosphaera*, *Leptolyngbya*, and *Microcoleus*. The bacterioplankton network consisted of 13 key genera, including *Erythrobacter*, *Rhodoferax*, *NovoSphingobium*, and *Haliscomenobacter*. The phytoplankton-bacterioplankton network comprises 17 key groups, primarily

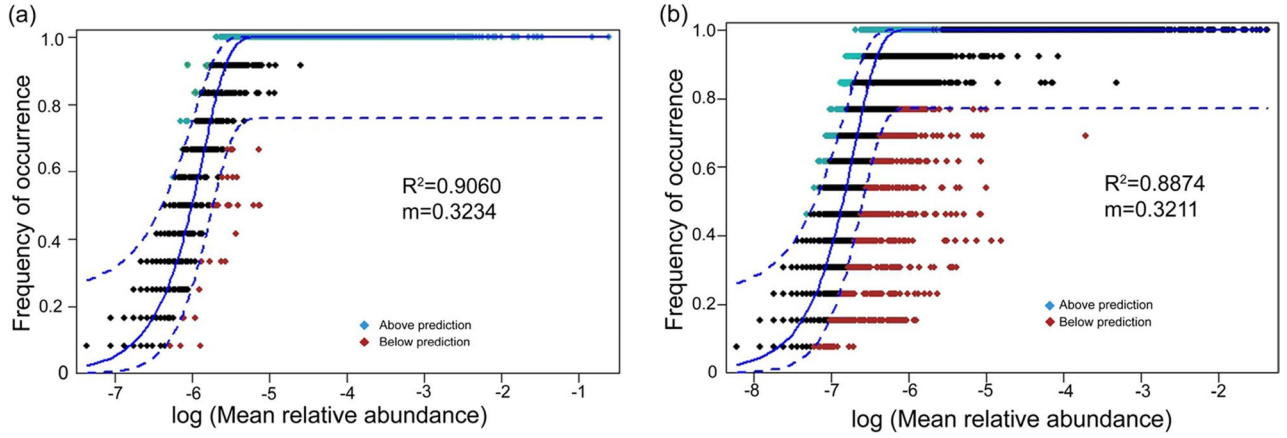

Fig. 3 The contribution of stochastic processes to the assembly of phytoplankton (**a**) and bacterioplankton (**b**) communities. R^2 represents the fit to the neutral model, and m indicates the immigration rate of the community. The points falling above and below the 95% confidence interval are colored cyan and orange, respectively, whereas those within the interval are colored black

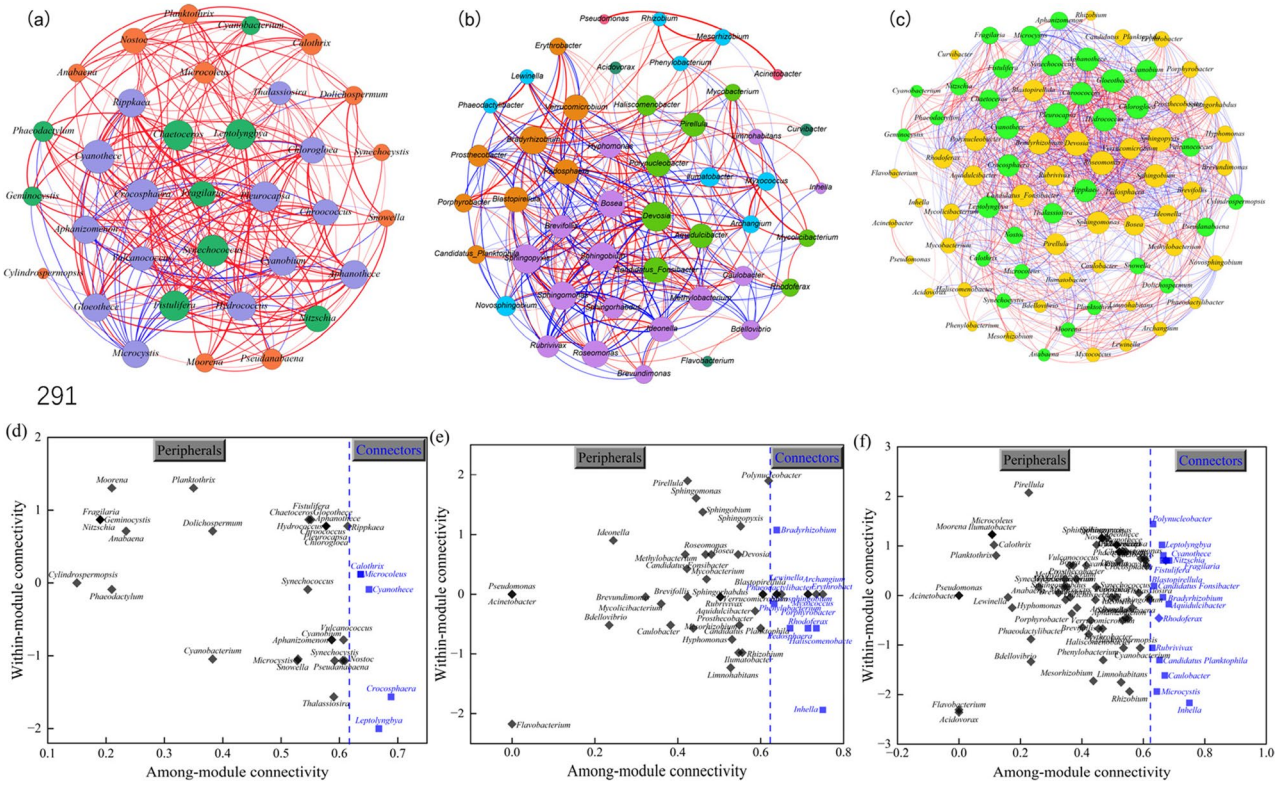

Fig. 4 Co-occurrence networks of phytoplankton (**a**), bacterioplankton (**b**), and phytoplankton-bacterioplankton (**c**) communities at the genus level in Caohai. Red lines represent positive interactions (co-occurrence) among genera, while blue lines represent negative interactions (co-exclusion). Nodes in networks (**a**) and (**b**) are colored according to modularity class, while nodes in network (**c**) are colored by kingdom (green for phytoplankton and orange for bacterioplankton). Edge width is proportional to the Pearson correlation coefficient. Topological roles of the network nodes, defined by within-module connectivity (Zi) and among-module connectivity (Pi), are shown for phytoplankton (**d**), bacterioplankton (**e**) and phytoplankton-bacterioplankton (**f**) communities

including *Cyanothece*, *Microcystis*, *Polynucleobacter*, and *Blastopirellula*.

The interactions between phytoplankton and bacterioplankton

Correlation analysis was conducted between all phyla of phytoplankton and the phyla of bacterioplankton with a relative abundance of more than 0.1% to examine their relationships, as shown in Fig. S3. The community structure of phytoplankton was significantly influenced by bacterioplankton. Specifically, Cyanophyta was significantly affected by both Armatimonadetes and Myxococcota. Chlorophyta exhibited a significant negative correlation with Bacteroidota and a significant positive correlation with Deinococcus-Thermus. Bacillariophyta and Euglenozoa were significantly affected by Armatimonadetes and Nitrospirae, respectively. Rhodophyta, Haptophyta, Charophyta, Cryptophyta, and Phaeophyta also showed significant correlations with Deinococcus-Thermus. The relationship between phytoplankton genera with a relative abundance exceeding 0.1% and the dominant phyla among the top 10 bacterioplankton is illustrated in Fig. 5. The total variation was 15.14, with explanatory variables accounting for 97.00%. The cumulative variance contribution rates for Axis 1 and Axis 2 were 52.62% and 25.47%, respectively. Armatimonadetes, Verrucomicrobia, and Bacteroidota had a highly significant influence on the community structure of phytoplankton ($P < 0.05$).

The niche overlap values of dominant phytoplankton and bacterioplankton ranged from 0.39 to 0.97 (Fig. 6a). Five pairs had overlap values less than 0.5, with the smallest being *Sphingomonas* and *Snowella* (0.39). Sixteen pairs had overlap values greater than 0.9, with the highest being *Rubrivivax* and *Microcystis* (0.97). The mean niche overlap value for dominant phytoplankton was 0.85, with 8 pairs having overlap values greater than 0.8, accounting for 53.33% of the total pairs. These pairs primarily included *Synechococcus* and *Cyanobium* (0.99), followed by *Thalassiosira* and *Synechococcus* (0.93). The average niche overlap value for dominant bacterioplankton was 0.91, with the minimum overlap value being between *Rubrivivax* and *Sphingomonas* (0.69), and the maximum overlap value between Brevundimonas and *Hyphomonas* (0.98). Among the correlations of dominant genera in phytoplankton and bacterioplankton (Fig. 6b),

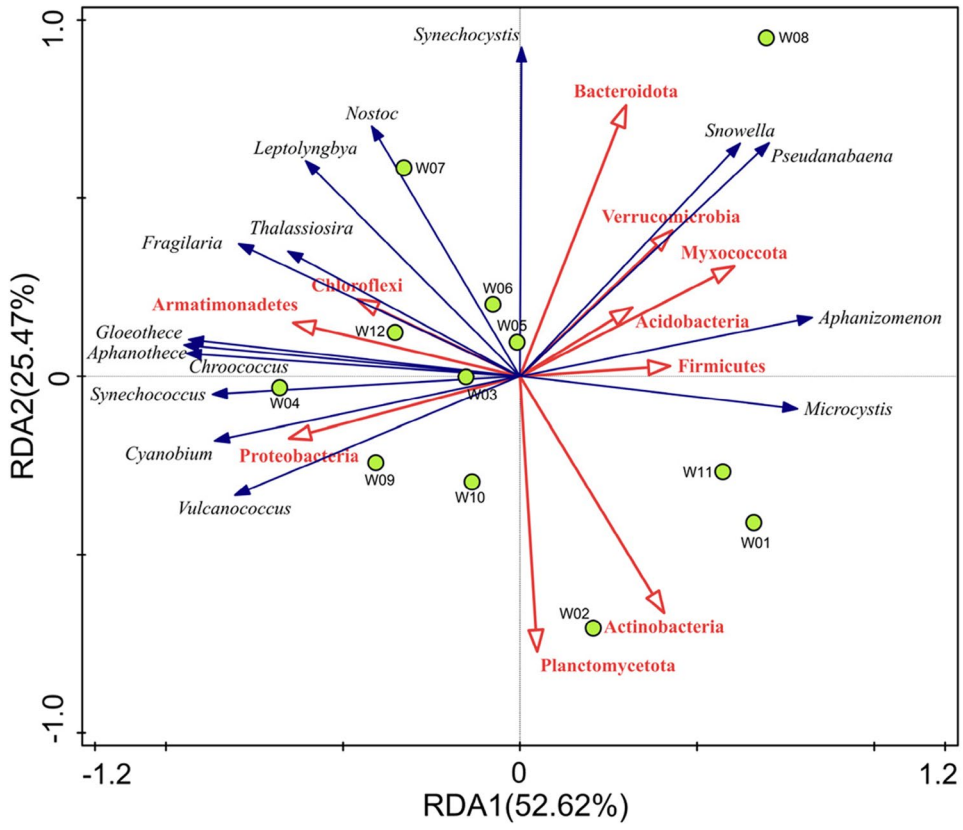

Fig. 5 RDA ordination plot illustrates the relationships between the phytoplankton community at the phylum level and the top 10 genera of the bacterioplankton

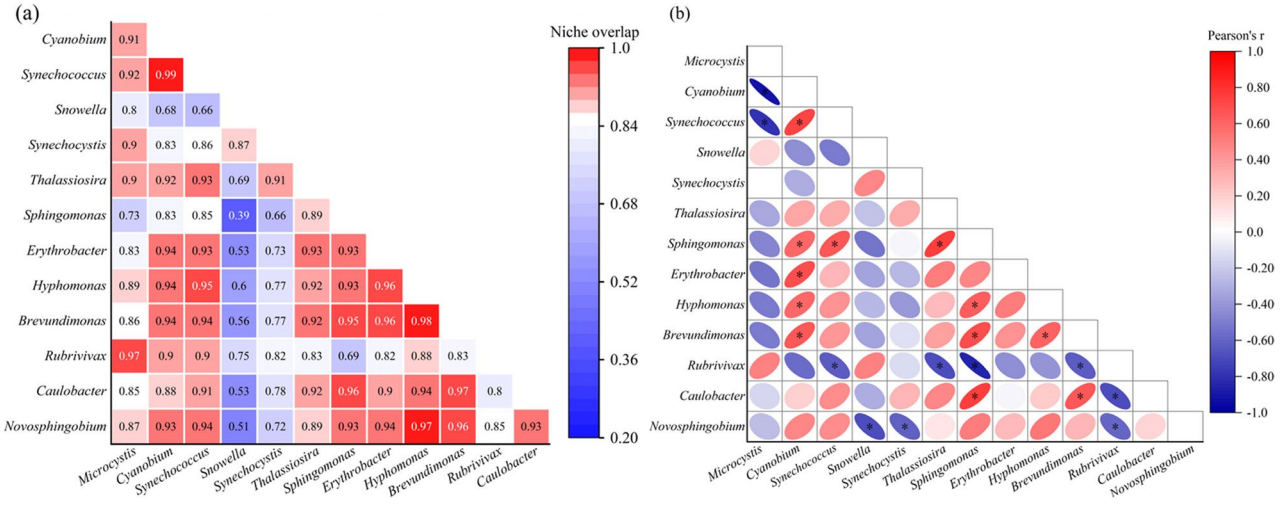

Fig. 6 (**a**) Niche overlap of dominant phytoplankton and bacterioplankton genera in Caohai. Colors closer to "red" indicate higher overlap values approaching "1", while colors closer to "blue" indicate lower overlap values approaching "0". (**b**) Pearson's correlation test of dominant phytoplankton and bacterioplankton genera in Caohai. Red color indicates a positive correlation, while blue color signifies a negative correlation

the positive and negative correlations were found to be equal (21 pairs). Among phytoplankton-bacterioplankton interactions, six pairs exhibited a significant positive correlation, whereas four pairs displayed a significant negative correlation. Among the correlations in the dominant phytoplankton, there was one pair of significant positive correlations and two pairs of negative correlations. Among correlations in the dominant bacterioplankton, there were five pairs of significant positive correlations and four pairs of negative correlations.

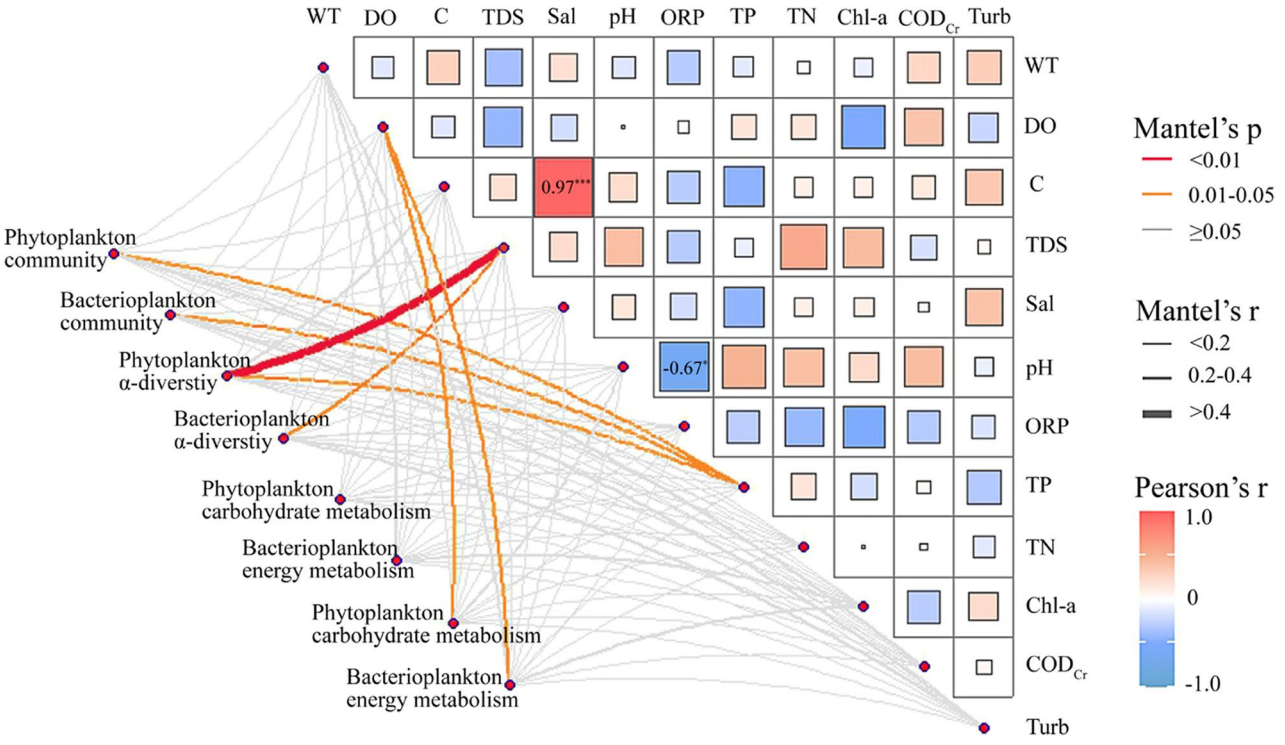

Fig. 7 Pairwise comparisons of environmental factors and phytoplankton and bacterioplankton at the genus level with a relative abundance of more than 0.1%, with a color gradient denoting Pearson's correlation coefficient. α-diversity indices were Chao1, Simpson and Shannon. Line width corresponds to the Mantel correlation coefficient, and the line color represents the statistical significance based on 9999 permutations

Mantel analysis was implemented to investigate the physicochemical factors that contributed most to the bacterioplankton and phytoplankton communities (Fig. 7). The results showed that TP was the key environmental factor affecting both the phytoplankton and bacterioplankton communities (genus level). The phytoplankton α-diversity index (Chao1, Simpson and Shannon) was mainly affected by TDS and TP, while the bacterioplankton α-diversity index was mainly affected by TP. The carbohydrate and energy metabolism pathways of bacterioplankton were significantly affected by DO, while the carbohydrate and energy metabolism pathways of phytoplankton were not significantly related to any environmental factors.

Discussion

Characteristics of community composition and metabolic pathways of phytoplankton and bacterioplankton in Caohai

This study revealed a diverse array of phytoplankton in Caohai through the use of eDNA method, identifying a total of 331 species belonging to 10 phyla and 197 genera. Cyanophyta (96.33%±1.09%) was the most dominant phylum, with *Microcystis* (40.43%±8.87%) being the most prevalent genus. Guo et al. [11] identified 7 phyla and 78 species of phytoplankton in Caohai through microscopy; among these, Cyanophyta exhibited the highest abundance during summer, and *Microcystis* was the dominant genus throughout the year. This indicates that eDNA detection revealed greater species diversity compared to traditional microscopic morphology methods, while remaining consistent in the dominant groups. The genera *Cyanobium* and *Synechococcus*, both micro-phytoplankton (< 2 μm), are widely distributed in freshwater systems and are challenging to accurately identify using morphological detection methods [46]. In this study, *Cyanobium* (12.31% ± 2.64%) and *Synechococcus* (8.90% ± 2.05%) were ranked as the second and third most abundant taxa, respectively, which indicated that eDNA technology could effectively overcome the limitations of morphological identification and detect small species with high sensitivity, thereby providing a more comprehensive understanding of phytoplankton community structure [23]. The relative abundance of *Microcystis* was notably high, exceeding 50% at two specific sampling sites, W1 and W11. These high concentrations were particularly concerning, especially during the summer months when temperatures rose. Elevated temperatures, nutrient-rich waters, and ample sunlight in Caohai collectively create an ideal environment for the rapid growth and proliferation of *Microcystis*. Microcystis blooms can have significant negative consequences, warranting heightened vigilance due to their ability to reduce water clarity and dissolved-oxygen levels, release toxic

microcystins, trigger fish kills, disrupt aquatic food webs, and ultimately endanger both water quality and public health [17]. Understanding the factors contributing to the dominance of *Microcystis* and Cyanobacteria blooms is crucial for maintaining ecological balance and ensuring water safety.

In Caohai, Proteobacteria, Bacteroidota, and Actinobacteria contributed more than 75% of all bacterioplankton (Fig. 1c). A similar trend was observed in the Yunnan-Guizhou Plateau, including Yangzong Lake, Chenghai Lake, and Erhai Lake, where Proteobacteria, Actinobacteria, and Bacteroidota were dominant [25, 26]. Similarly, the results of bacterial communities in 21 plateau lakes of China showed that Proteobacteria was the most abundant phylum, followed by Bacteroidota and Actinobacteria [22]. Proteobacteria have been reported to contribute to nitrogen fixation, photosynthesis, sulfur metabolism, methane metabolism, and can also degrade proteins, polysaccharides and other organic matter as well as remove these compounds [20]. Actinobacteria play a vital role in the complex process of carbon cycling within aquatic ecosystems [28]. Thus, both groups play essential roles in material cycling in lake planktonic ecosystems, thereby significantly supporting ecosystem stability. *Sphingomonas* was the genus exhibiting the highest relative abundance among the bacterioplankton in Caohai, which are widely distributed in soils, fresh, marine waters, plants, and other environmental media [19]. It is capable of efficiently degrading phycotoxins and organic compounds, and actively breaking down toxins associated with *Microcystis* [4].

The bacterioplankton in Caohai were primarily composed of heterotrophic bacteria, with a smaller proportion being photosynthetic autotrophic bacteria. A clear distinction in carbohydrate metabolism and energy metabolism was observed between phytoplankton and bacterioplankton (Fig. 2a), which seemed primarily associated with the specificities of autotrophic versus heterotrophic metabolic pathways [12]. LEfSe analysis disclosed that the phytoplankton exhibited significant functional activity related to photosynthesis, photosynthesis antenna proteins, and starch and sucrose metabolisms (Fig. 2b), while the bacterioplankton mostly presented activity in propanoate metabolism, butanoate metabolism, glyoxylate and dicarboxylate metabolism, and TCA cycle. This illustrates the overall metabolic complementation that exists between phytoplankton and bacterioplankton. In this study, the methane metabolic pathway was found to be highly abundant in both phytoplankton and bacterioplankton. Higher trophic status increases the biomass of phytoplankton and bacterioplankton [45]. Under eutrophication, these elevated biomass levels generate hypoxic or anaerobic conditions that facilitate the long-term production and emission of CH_4 in Caohai [44].

The assembly mechanisms of phytoplankton and bacterioplankton in Caohai

The NCM model can predict the relative importance of deterministic and stochastic processes in community assembly [53]. The R^2 values of the NCM model for the phytoplankton community exceeded 90%, indicating that phytoplankton community assembly was primarily driven by stochastic processes in Chaohai. Many bacterioplankton taxa were not well explained by the NCM model, suggesting a stronger influence of deterministic processes. Given the lake's rapid internal water mixing, dispersal limitation is considered unlikely. Instead, the strong stochastic signal suggests that demographic drift and other random in-lake processes are the primary drivers of community assembly. Some studies have found that stochastic factors exerted a more pronounced influence on the fluctuations of microbial communities at relatively small spatial scales, while deterministic factors have a more significant impact on the fluctuations of microbial communities at larger spatial scales [43]. In Caohai, the assembly of phytoplankton and bacterioplankton communities was primarily influenced by stochastic factors, likely due to its limited spatial scale. Caohai, a shallow freshwater lake located on the Yunnan-Guizhou Plateau, had limited connectivity to other water bodies [27]. These characteristics created unique conditions that favor stochastic processes over deterministic ones.

The effects of environmental factors on these communities should not be overlooked. Many studies have examined environmental influences on microbial community structure from a deterministic perspective [54]. In contrast, other studies have found that environmental factors such as total TN and DO can influence the relative importance of stochastic processes [31]. The TN and TP concentrations in Caohai were 1.99 ± 0.21 mg/L and 0.10 ± 0.02 mg/L, respectively (Table S1), indicating that Caohai had been degraded to a mesotrophic or eutrophic state based on China's Environmental Quality Standards for Surface Water (GB3838–2002). While stochastic processes might dominate in Caohai, environmental conditions still play a crucial role in shaping the overall structure and function of the biological communities. The Mantel analysis showed that TP was the main environmental factor influencing the phytoplankton and bacterioplankton community in Caohai. This was consistent with the results of Wen et al. [50], who reported that TP was the main driver of phytoplankton in Lijiahe Reservoir. Jiang et al. [16] also found that P might be the primary limiting factor for phytoplankton growth under sufficient nutrient conditions. The TP content in Caohai was high during the summer season, facilitating

unrestricted reproduction and growth of phytoplankton and bacterioplankton communities. High TP levels in Caohai reduce environmental selection pressure, thereby allowing stochastic processes to become dominant. Previous studies have reported that elevated nutrients could alleviate environmental selection pressures by augmenting resource availability in aquatic systems, leading to a reduction in interspecific competition and an increased significance of stochastic processes in community assembly [7]. Consistent with this, the high TP concentrations in Caohai appear to have promoted stochasticity in the assembly of phytoplankton and bacterioplankton communities. The Mantel analysis revealed that the energy and carbon metabolism of bacterioplankton were primarily influenced by DO (Fig. 7). This remarkable finding suggests that aerobic respiration assumes a preponderant and critical role in the complex metabolic processes of bacterioplankton [9]. It indicates that the availability and concentration of dissolved oxygen profoundly influence how bacterioplankton perform their essential metabolic functions.

Co-occurrence network analysis was employed to elucidate species interactions and their impact on community assembly, thereby complementing the biological factors in the community assembly. In the phytoplankton network, 84.25% of the interactions were positive (Fig. 4a), as inferred from Pearson correlation coefficients, indicating that mutualistic or symbiosis relationships predominate among phytoplankton species. Notably, some positive correlation coefficients also mean that taxa responded similarly to environmental conditions without direct interactions among them. In contrast, in the bacterioplankton network, the number of positive interactions was nearly equal to that of negative interactions (51.51% vs. 48.49%, Fig. 4b). In a co-occurrence network, the topological characteristics of graph density (D)/clustering coefficient (CC) could serve as an indicator of network stability [54]. The D/CC value of the phytoplankton network was 0.626, higher than that of the bacterioplankton network (0.537), indicating that the phytoplankton community structure was more stable compared to the bacterioplankton community. The key taxa exhibiting high connectivity in the network played a crucial role in upholding the stability of the microbial network [54]. The impact of key taxa on the community structure in co-occurrence networks is not determined by their relative abundance but by their strong ecological associations [42]. In the phytoplankton network, *Cyanothece* had the highest number of edges and exerted a significant influence on other phytoplankton. *Cyanothece* carries out photosynthesis during the daytime, transforming sunlight into chemical energy. Subsequently, nitrogen fixation occurs as oxygen levels decrease due to nocturnal respiration [24]. This sequential process plays a crucial role in maintaining the ecological balance and functionality within the phytoplankton community. *Sphingobium* and *Sphingopyxis* were identified as key taxa within the bacterioplankton network. Notably, these two genera have been previously well-documented in numerous scientific studies for their remarkable capacity to effectively degrade microcystins [49]. This degradation ability is of significant importance in eutrophic lake ecosystems, as microcystins can pose serious threats to the stability and health of aquatic ecosystems. In addition, in diverse and complex ecosystems, *Sphingobium* plays an extremely crucial role in the meticulous process of organic matter decomposition and actively participates in the cycling of essential elements such as nitrogen and phosphorus [29]. Through their significant contributions, *Sphingobium* and *Sphingopyxis* effectively contribute to maintaining the delicate and vital ecological equilibrium.

The interactions between phytoplankton and bacterioplankton in Caohai

Previous studies of phytoplankton in Caohai primarily focused on the species composition and community function of phytoplankton. Given that the phytoplankton and bacterioplankton communities are closely interconnected, these studies were far from sufficient to thoroughly understand and repair the aquatic ecosystem affected by phytoplankton [55]. The interactions between bacterioplankton and phytoplankton in aquatic ecosystems were complex and idiosyncratic, involving processes that can be either positive or negative [34]. This study found that the abundance and community composition of bacterioplankton were significantly correlated with the abundance of phytoplankton, in which Cyanophyta had a highly significant influence on the community structure of bacterioplankton. In the Erhai survey, it was found that the abundance and community composition of bacterioplankton were significantly correlated with the abundance of phytoplankton [15]. Zhang et al. [55] found in their study of Dianchi Lake that the structure of the phytoplankton community has a significant impact on the abundance of bacterioplankton, among which Cyanobacteria have the greatest influence on the composition of planktonic bacteria. The photosynthesis-derived carbon generated by Cyanophyta was actively exported and subsequently formed a thick and substantial extracellular polymeric substance (EPS) [35]. This substantial EPS is likely to provide a crucial source of nourishment and fuel the growth of heterotrophic bacteria that have the ability to utilize these specific compounds [12]. Correlation analysis revealed a negative association between *Microcystis* and the majority of dominant phytoplankton and bacterioplankton (Fig. 6b). This phenomenon might be closely related to the inherent ability of *Microcystis* to secrete microcystin, which has been suggested

to be potential allelochemicals that have a counteractive effect against other phytoplankton and aquatic organisms [17]. Bacteroidota had a highly significant influence on the community structure of phytoplankton revealed by RDA analysis (Fig. 5b). Some studies have found that Bacteroidota might potentially play a vital and indispensable role in the meticulous processing of organic matter throughout the entire process of algal blooms [37].

Co-occurrence network analysis revealed that positive interactions were more prevalent than negative interactions between phytoplankton and bacterioplankton (Fig. 4c). When combined with the metabolic specialization and complementarity of these two groups as revealed by LEfSe analysis (Fig. 2b), the findings suggested that mutualistic relationships were more prevalent than competitive ones in the phytoplankton-bacterioplankton interactions within Caohai. Phytoplankton specialized in photosynthesis and carbon storage, while bacterioplankton dominated anaerobic respiration (propanoate metabolism). Planktonic heterotrophic bacteria acquire significant carbon requirements directly from phytoplankton, with up to 50% of the carbon fixed by phytoplankton eventually being consumed by bacteria. While bacterioplankton can provide limited nutrients to phytoplankton through mineralization, they also compete for inorganic nutrients [41]. This complex interaction and balance between these two processes play a crucial role in shaping the overall dynamics and stability of the lake ecosystem. In the phytoplankton-bacterioplankton network, *Rubrivivax* and *Polynucleobacter* interacted with 61.76% of phytoplankton, with the majority of these interactions characterized as negative. Specifically, *Rubrivivax*, classified as a denitrifying bacterium [33], could convert nitrate (NO_3-N) in water into nitrogen gas (N_2). This process created competition with phytoplankton for the essential nutrient. Additionally, *Polynucleobacter* possesses the capability of decomposition and transformation of protein-rich dissolved organic matter derived from algae [56].

The predominance of positive interactions between phytoplankton and bacterioplankton in Caohai (Fig. 4c) may be attributed to eutrophication, which is characterized by nutrient abundance and minimal interspecific resource competition. Niche overlap indicates the degree of similarity in resource utilization (e.g., food, habitat) among species. A high niche overlap does not necessarily indicate intense interspecific competition, as niche overlap is a necessary but insufficient condition for such competition [1]. Unless two (or more) sympatric populations share a resource that limits population size, interspecific competition is unlikely to occur [47]. Niche overlap and interspecific correlation often result from shared resource use among genera, and there is a certain relationship between them. This study found that genus pairs with high positive correlations exhibited correspondingly higher niche overlap values. Conversely, genus pairs with high negative correlations showed lower niche overlap values. Several studies have demonstrated that a higher degree of positive interspecific association correlates with greater niche overlap [18]. Pastore et al. [32] discovered that niche overlap leads to more coexistence in expansive environments. In this study, the high niche overlap value and positive correlation between the genus pairs might be related to the expansive environment and abundant nutrients (such as N and P) in the Caohai area. Tang et al. [45] discovered that the increase in the trophic state enhanced the interaction between phytoplankton and bacterial communities, and the negative links in the eutrophic network were fewer than those in the oligotrophic and mesotrophic networks.

Research limitations and prospects

This study employed eDNA metagenomics to achieve a more comprehensive understanding of phytoplankton biodiversity, functional characteristics, and species interactions compared to conventional methodologies [10], and provided foundational insights into the mechanisms underlying interactions between phytoplankton and bacterioplankton. Nevertheless, these advantages are constrained by factors such as the reproducibility of DNA extraction, sequencing depth, and the efficacy of bioinformatic analysis pipelines [38], as well as by certain temporal and spatial limitations. To address these constraints, future research will implement a nested experimental design, whereby each water sample will be divided into a minimum of three independent DNA extraction replicates, each subjected to multiple rounds of PCR amplification and DNA sequencing. This approach aims to enhance experimental reproducibility and data reliability. Additionally, complementary techniques such as microscopic identification and metabarcoding will be employed for cross-validation, while improvements in sequencing depth and optimization of assembly algorithms will be pursued to increase result accuracy.

While the study captures community interaction patterns during the peak of eutrophication, the single spatiotemporal snapshot limits the generalizability of the findings. To strengthen the robustness and broader relevance of the conclusions, future research should extend to plateau lakes across broader spatiotemporal scales, encompassing systems with varying trophic states and incorporating long-term spatiotemporal monitoring that integrates data on seasonal and interannual variability. This will enable rigorous validation of key findings, such as the dominance of stochastic processes in community assembly and the positive interaction, across diverse eutrophic plateau lake ecosystems.

Conclusion

The high concentrations of TN and TP in Caohai led to its eutrophic state, and contributed to the rich phytoplankton community. Metagenomics-based eDNA provided a more sensitive and comprehensive characterization of the phytoplankton community compared to traditional morphology-based approaches, while remaining consistent in the dominant groups. Cyanophyta was identified as the dominant phylum, with *Microcystis* being the predominant genus. Heightened vigilance is required to mitigate the risk of algal blooms.

Due to nutrient enrichment, relatively uniform environmental conditions, and the limited spatial scale in Caohai, the assembly patterns of phytoplankton and bacterioplankton communities were predominantly influenced by stochastic processes. Additionally, environmental factors (TP and DO), interspecies interactions, and key taxa (such as *Cyanothece*, *Sphingobium*) also played significant roles in shaping community assembly and stability.

The abundance and community composition of bacterioplankton in Caohai were significantly correlated with the abundance of phytoplankton. The mutualistic interactions (positive effect) between phytoplankton and bacterioplankton were stronger than their competitive ones (negative effect). High niche overlap values and positive correlation between phytoplankton and bacterioplankton were observed in Caohai, which might be attributed to the expansive environment, abundant nutrients, metabolic complementarity and less competition for resources among organisms. Nevertheless, the phytoplankton-bacterioplankton interaction mechanisms identified in this study require validation across multiple lakes and seasons, and their generalizability requires broader-scale research.

Supplementary Information

The online version contains supplementary material available at https://doi.org/10.1186/s12866-025-04536-w.

Supplementary Material 1.

Acknowledgements
This work was financially supported by Guizhou Provincial Science and Technology Projects, China (QKHJC-ZK[2023]YB233, QKHPT[2025]015), National Natural Science Foundation of China (32360036), Talent Team Project of Guizhou Institute of Biology, China (QSS2024001).

Authors' contributions
Jin Guo: Conceptualization, Methodology, Software, Formal analysis, Data curation, Validation, Writing - original draft. Liangliang Dai: Investigation, Data curation, Software. Juan Jiang: Validation, Writing - review & editing. Yunchuan Long: Conceptualization, Investigation, Resources, Visualization, Supervision, Writing - review & editing. All authors reviewed the manuscript.

Funding
This work was financially supported by Guizhou Provincial Science and Technology Projects, China (QKHJC-ZK[2023]YB233, QKHPT[2025]015), National Natural Science Foundation of China (32360036), Talent Team Project of Guizhou Institute of Biology, China (QSS2024001).

Data availability
The raw sequences have been deposited in the NCBI Sequence Read Archive (SRA) database under BioProject PRJNA1243597 (accession number SAMN47626520 to SAMN47626531) and are publicly available.

Declarations

Ethics approval and consent to participate
Not applicable.

Consent for publication
Not applicable.

Competing interests
The authors declare no competing interests.

Author details
[1]Guizhou Key Laboratory of Plateau Wetland Conservation and Restoration, Guizhou Institute of Biology, Guiyang 550009, People's Republic of China
[2]Caohai Ecological Research Station, Guizhou Academy of Sciences, Weining 553100, People's Republic of China

Received: 5 June 2025 / Accepted: 6 November 2025
Published online: 05 January 2026

References

1 Chesson P. Ecological niches and diversity maintenan. Department Ecol Evolutionary Biology. 2011;10:43–60.
2 Chua PYS, Crampton-Platt A, Lammers Y, Alsos IG, Boessenkool S, Bohmann K. Metagenomics: a viable tool for reconstructing herbivore diet. Mol Ecol Resour. 2021;21(7):2249–63.
3 Cole JJ. Interactions between bacteria and algae in aquatic ecosystems. Annu Rev Ecol Syst. 1982;13(1):291–314.
4 Cook KV, Li C, Cai H, Krumholz LR, Hambright KD, Paerl HW, Steffen MM, Wilson AE, Burford MA, Grossart HP, Hamilton DP, Jiang H, Sukenik A, Latour D, Meyer EI, Padisák J, Qin B, Zamor RM, Zhu G. The global *Microcystis* interactome. Limnol Oceanogr. 2020;65:S194–207.
5 Costas-Selas C, Martínez-García S, Delgadillo-Nuño E, Justel-Díez M, Fuentes-Lema A, Fernández E, Teira E. Linking the impact of bacteria on phytoplankton growth with microbial community composition and co-occurrence patterns. Mar Environ Res. 2024;193:106262.
6 Ding Y, Pan B, Han X, Guo S, Feng Z, Sun H, et al. Habitat selection drives diatom community assembly and network complexity in sediment-laden riverine environments. Sci Total Environ. 2024;934:172983.
7 Fang W, Fan T, Wang S, Yu X, Lu A, Wang X, et al. Seasonal changes driving shifts in microbial community assembly and species coexistence in an urban river. Sci Total Environ. 2023;905:167027.
8 Faure E, Ayata S-D, Bittner L. Towards omics-based predictions of planktonic functional composition from environmental data. Nat Commun. 2021;12:4361.
9 Grossart HP, Massana R, McMahon KD, Walsh DA. Linking metagenomics to aquatic microbial ecology and biogeochemical cycles. Limnol Oceanogr. 2019;65:S2–20.
10 Guo J, Dai LL, Jiang J, Long YC. Responses of phytoplankton communities to human activities in lake Caohai wetland based on environmental DNA metagenome. J Lake Sci. 2025;37(4):1151–61.
11 Guo Y, Xu Y, Li R, Zhou C, Du M, Liu K. Phytoplankton community structure and its relationship with environmental factors in Caohai Lake, Guizhou, China. Asian Journal of Eeotoxicology. 2024;19(3):306–18.

12 Halary S, Duperron S, Demay J, Duval C, Hamlaoui S, Piquet B, Reinhardt A, Bernard C, Marie B. Metagenome-based exploration of bacterial communities associated with cyanobacteria strains isolated from thermal muds. Microorganisms. 2022;10(12):2337.
13 Han X, Pan B, Jin X, Li M, Ding Y, Liu X. The assembly mechanisms of algal community across different habitats mediated by sediment in the heavily sediment-laden Yellow River. J Hydrol. 2024;631:130825.
14 Huang Z, Pan B, Zhao X, Liu X, Liu X, Zhao G. Hydrological disturbances enhance stochastic assembly processes and decrease network stability of algae communities in a highland floodplain system. Sci Total Environ. 2023;903:166207.
15 Hu MM, Li YH, Wang YC, Zhou HD, Liu YD, Zhao GF. Phytoplankton and bacterioplankton abundances and community dynamics in lake Erhai. Water Sci Technol. 2013;68(2):348–56.
16 Jiang M, Nakano S-i. The crucial influence of trophic status on the relative requirement of nitrogen to phosphorus for phytoplankton growth. Water Res. 2022;222:118868.
17 Jin H, Ma H, Gan N, Wang H, Li Y, Wang L, et al. Non-targeted metabolomic profiling of filamentous cyanobacteria *Aphanizomenon flos-aquae* exposed to a concentrated culture filtrate of *Microcystis* aeruginosa. Harmful Algae. 2022;111:102170.
18 Juan W, Junjie L, Chao L, Xiaoyu D, Yong W. Species niche and interspecific associations alter flora structure along a fertilization gradient in an alpine meadow of Tianshan Mountain, Xinjiang. Ecol Indic. 2023;147:109953.
19 Kopejtka K, Zeng Y, Kaftan D, Selyanin V, Gardian Z, Tomasch J, et al. Characterization of the aerobic anoxygenic phototrophic bacterium *Sphingomonas* sp. AAP5. Microorganisms. 2021;9(4):768.
20 Kuang B, Xiao R, Hu Y, Wang Y, Zhang L, Wei Z, Bai J, Zhang K, Acuña JJ, Jorquera MA, Pan W. Metagenomics reveals biogeochemical processes carried out by sediment microbial communities in a shallow eutrophic freshwater lake. Front Microbiol. 2023;13:1112669.
21 Li A, Huang X, Tian Y, Dong J, Zheng F, Xia P. Chlorophyll a variation and its driving factors during phase shift from macrophyte-to phytoplankton-dominated states in Caohai Lake, Guizhou, China. Chin J Plant Ecol. 2023;47(8):1171–81.
22 Liao J, Cao X, Zhao L, Wang J, Gao Z, Wang MC, et al. The importance of neutral and niche processes for bacterial community assembly differs between habitat generalists and specialists. FEMS Microbiol Ecol. 2016;92(11):fiw174.
23 Lin Y, Shen L, Xu S, Zhou X, He L, Zhao Z. Impacts of anthropogenic activities on eukaryotic phytoplankton communities in Panlong river via eDNA biomonitoring. Hydrobiologia. 2024;851:4007–18.
24 Liu D, Liberton M, Yu J, Pakrasi HB, Bhattacharyya-Pakrasi M, Papoutsakis ET, Bricker T, Sherman L. Engineering nitrogen fixation activity in an oxygenic phototroph. mBio. 2018;9(3):e01029–01018.
25 Liu Q, Chang F, Xie P, Zhang Y, Duan L, Li H, Zhang X, Zhang Y, Li D, Zhang H. Microbiota assembly patterns and diversity of nine plateau lakes in Yunnan, Southwestern China. Chemosphere. 2023;314:137700.
26 Liu Q, Zhang H, Zhang Y, Li D, Gao Y, Li H, et al. Heterogeneous bacterial communities affected by phytoplankton community turnover and microcystins in plateau lakes of Southwestern China. Sci Total Environ. 2023;903:166303.
27 Long Y, Jiang J, Hu X, Hu J, Ren C, Zhou S. The response of microbial community structure and sediment properties to anthropogenic activities in Caohai wetland sediments. Ecotoxicol Environ Saf. 2021;211:111936.
28 Mikhailov IS, Zakharova YR, Bukin YS, Galachyants YP, Petrova DP, Sakirko MV, Likhoshway YV. Co-occurrence networks among bacteria and microbial eukaryotes of lake Baikal during a spring phytoplankton bloom. Microb Ecol. 2018;77(1):96–109.
29 Mishra S, Lin Z, Pang S, Zhang W, Bhatt P, Chen S. Recent advanced technologies for the characterization of xenobiotic-degrading microorganisms and microbial communities. Front Bioeng Biotechnol. 2021;9:632059.
30 Monchamp MÈ, Walsh DA, Garner RE, Kraemer SA, Beisner BE, Cristescu ME, Gregory-Eaves I. Comparative analysis of zooplankton diversity in freshwaters: what can we gain from metagenomic analysis? Environ DNA. 2022;4(6):1250–64.
31 Niu S, Xie J, Wang G, Li Z, Zhang K, Li H, et al. Community assembly patterns and processes of bacteria in a field-scale aquaculture wastewater treatment system. Sci Total Environ. 2024;907:167913.
32 Pastore AI, Barabás G, Bimler MD, Mayfield MM, Miller TE. The evolution of niche overlap and competitive differences. Nat Ecol Evol. 2021;5(3):330–7.
33 Paver SF, Hayek KR, Gano KA, Fagen JR, Brown CT, Davis-Richardson AG, Crabb DB, Rosario-Passapera R, Giongo A, Triplett EW, Kent AD. Interactions between specific phytoplankton and bacteria affect lake bacterial community succession. Environ Microbiol. 2013;15(9):2489–504.
34 Peng X, Fanxiang K, Huansheng C, Min Z. Relationship between bacterioplankton and phytoplankton community dynamics during late spring and early summer in lake Taihu, China. Acta Ecol Sin. 2007;27(5):1696–702.
35 Pereira S, Mota R, Vieira C, Vieira J, Tamagnini P. Phylum-wide analysis of genes/proteins related to the last steps of assembly and export of extracellular polymeric substances (EPS) in Cyanobacteria. Sci Rep. 2015;5:14835.
36 Pikitch EK. A tool for finding rare marine species. Science. 2018;360(6394):1180–2.
37 Pinhassi J, Sala MM, Havskum H, Peters F, Guadayol Ò, Malits A, Marrasé C. Changes in bacterioplankton composition under different phytoplankton regimens. Appl Environ Microbiol. 2004;70(11):6753–66.
38 Rocha U, Kasmanas JC, Toscan R, Sanches DS, Magnusdottir S, Saraiva JP. Simulation of 69 microbial communities indicates sequencing depth and false positives are major drivers of bias in prokaryotic metagenome-assembled genome recovery. PLoS Comput Biol. 2024;20(10):e1012530.
39 Schulte NO, Craine JM, Leopold DR, Devitt JK, Fierer N. Diversity of freshwater algal assemblages across the United States as revealed by DNA metabarcoding. Environ DNA. 2023;6:e477.
40 Serite CP, Emami-Khoyi A, Ntshudisane OK, James NC, van Jansen Vuuren B, Bodill T, et al. eDNA metabarcoding vs metagenomics: an assessment of dietary competition in two estuarine pipefishes. Front Mar Sci. 2023;10:1116741.
41 Seymour JR, Amin SA, Raina J-B, Stocker R. Zooming in on the phycosphere: the ecological interface for phytoplankton–bacteria relationships. Nat Microbiol. 2017;2(7):17065.
42 Shi L, Xia P, Lin T, Li G, Wang T, Du X. Temporal succession of bacterial community structure, co-occurrence patterns, and community assembly process in epiphytic biofilms of submerged plants in a plateau lake. Microb Ecol. 2022;85(1):87–99.
43 Shi Y, Li Y, Xiang X, Sun R, Yang T, He D, Zhang K, Ni Y, Zhu Y-G, Adams JM, Chu H. Spatial scale affects the relative role of stochasticity versus determinism in soil bacterial communities in wheat fields across the North China plain. Microbiome. 2018;6(1):27.
44 Sun HY, Lu XX, Yu RY, Yang J, Liu XY, Cao ZX, et al. Eutrophication decreased CO2 but increased CH4 emissions from lake: a case study of a shallow Lake Ulansuhai. Water Res. 2021;201:117363.
45 Tang Q, Lu L, Luo F, Li X, Zhang Y, Li R, et al. Terrigenous organic carbon contributes to reservoir carbon emissions: potential role of the microbial community along a trophic gradient. J Hydrol. 2023;621:129601.
46 Te SH, Kok JWK, Luo R, You L, Sukarji NH, Goh KC, et al. Coexistence of *Synechococcus* and *Microcystis* blooms in a Tropical Urban Reservoir and their links with microbiomes. Environ Sci Technol. 2023;57(4):1613–24.
47 Thomas R, A. Competition theory, evolution, and the concept of an ecological niche. Acta Biotheor. 1982;31:165–79.
48 Wang H, Zhu R, Zhang X, Li Y, Ni L, Xie P, Shen H. Abiotic environmental factors override phytoplankton succession in shaping both free-living and attached bacterial communities in a Highland lake. AMB Express. 2019;9:170.
49 Wei J, Pengji Z, Zhang J, Peng T, Luo J, Yang F. Biodegradation of MC-LR and its key bioactive moiety Adda by *Sphingopyxis* sp. YF1: comprehensive elucidation of the mechanisms and pathways. Water Res. 2023;229:119397.
50 Wen C, Huang T, Wen G, Li K, Yang S, Zhang H, Xu J, Wang Z. Controlling phytoplankton blooms in a canyon-shaped drinking water reservoir via artificial and induced natural mixing: taxonomic versus functional groups. Chemosphere. 2022;287:131771.
51 Wu S, Dong Y, Stoeck T, Wang S, Fan H, Wang Y, et al. Geographic characteristics and environmental variables determine the diversities and assembly of the algal communities in interconnected river-lake system. Water Res. 2023;233:119792.
52 Yang C, Zhao Y, Cao W, Xing M, Xu X, Wang Z, et al. Metagenomic analysis reveals antibiotic resistance genes and virulence factors in the saline-alkali soils from the Yellow River Delta, China. Environ Res. 2022;214:113823.
53 Zeng L, Wen J, Huang B, Yang Y, Huang Z, Zeng F, et al. Environmental DNA metabarcoding reveals the effect of environmental selection on phytoplankton community structure along a subtropical river. Environ Res. 2024;243:117708.

54 Zhang H, Xu Y, Liu X, Ma B, Huang T, Kosolapov DB, et al. Different seasonal dynamics, ecological drivers, and assembly mechanisms of algae in southern and northern drinking water reservoirs. Sci Total Environ. 2024;922:171285.
55 Zhang Y, Zuo J, Salimova A, Li A, Li L, Li D. Phytoplankton distribution characteristics and its relationship with bacterioplankton in dianchi lake. Environ Sci Pollut Res Int. 2020;27(32):40592–603.
56 Zhou L, Wu Y, Zhou Y, Zhang Y, Xu H, Jang K-S, et al. Terrestrial dissolved organic matter inputs drive the temporal dynamics of riverine bacterial ecological networks and assembly processes. Water Res. 2024;249:120955.
57 Zhu J, Chen G, Zhou J, Zeng Y, Cheng K, Cai Z. Dynamic patterns of quorum sensing signals in phycospheric microbes during a marine algal bloom. Environ Res. 2022;212:113443.

Publisher's Note